THE JOURNAL OF BIOLOGICAL CHEMISTRY VOL. 288, NO. 17, pp. 12161–12174, April 26, 2013
© 2013 by The American Society for Biochemistry and Molecular Biology, Inc. Published in the U.S.A.

Negative Regulation of 26S Proteasome Stability via Calpain-mediated Cleavage of Rpn10 Subunit upon Mitochondrial Dysfunction in Neurons*

Received for publication, February 25, 2013 Published, JBC Papers in Press, March 18, 2013, DOI 10.1074/jbc.M113.464552

Qian Huang (黄倩)[‡1], Hu Wang (王虎)[‡1], Seth W. Perry[§], and Maria E. Figueiredo-Pereira[‡2]

From the [‡]Department of Biological Sciences, Hunter College and Graduate Center, City University of New York, New York, New York 10065 and the [§]Department of Biomedical Engineering, University of Rochester, Rochester, New York 14627

Background: Proteasomal and mitochondrial dysfunction are implicated in neurodegeneration.
Results: Upon mitochondrial dysfunction in neurons, calpain-mediated cleavage of Rpn10 negatively regulates 26S proteasome stability.
Conclusion: ATP deficiency and calpain-activation impair the ubiquitin/proteasome pathway with a concomitant increase in 20S proteasomes.
Significance: This proteolytic switch could promote degradation of randomly unfolded oxidized proteins in an unregulated and energy-independent manner by 20S proteasomes.

Proteasomal and mitochondrial dysfunctions are implicated in chronic neurodegenerative diseases. To investigate the impact of mitochondrial impairment on the proteasome, we treated rat cerebral cortical neurons with oligomycin, antimycin, or rotenone, which inhibit different elements of the electron transport chain. Firstly, we observed a reduction in ubiquitinated proteins and E1 activity. Secondly, we established that 26S proteasomes are disassembled with a decline in activity. Thirdly, we show, to our knowledge for the first time, that calpain activation triggers the selective processing of the 26S proteasome subunit Rpn10. Other proteasome subunits tested were not affected. Calpain also cleaved caspase 3 to an inactive fragment, thus preventing apoptosis that is an energy-dependent cell death pathway. In addition, calpain cleaved the microtubule-associated protein Tau, a major component of neurofibrillary tangles in Alzheimer disease and other tauopathies. Fourthly, we detected a rise in 20S proteasome levels and activity. Finally, we show that both acute (16 h) and long term (up to 7 days) mitochondrial impairment led to down-regulation of ubiquitinated-proteins, 26S proteasome disassembly, and a rise in 20S proteasomes. We postulate that upon mitochondrial dysfunction, ATP depletion and calpain activation contribute to the demise of protein turnover by the ubiquitin/proteasome pathway. The concomitant rise in 20S proteasomes, which seem to degrade proteins in an unregulated and energy-independent manner, in the short term may carry out the turnover of randomly unfolded oxidized proteins. However, if chronic, it could lead to neurodegeneration as regulated protein degradation by the ubiquitin/proteasome pathway is essential for neuronal survival.

Proteasome function is essential for neuronal homeostasis and survival. Neurons are also critically dependent on mitochondria for energy production necessary for maintaining homeostasis, neurotransmission, and plasticity. There is a mutual dependence between mitochondrial and proteasomal function (1). Mitochondria provide ATP required for 26S proteasomal degradation of ubiquitinated proteins, some of which are mitochondrial proteins. Emerging evidence implicates proteasomal and mitochondrial dysfunction in aging and neurodegenerative disorders such as Alzheimer disease (AD)[3] (2, 3). In neurons, this is particularly important because, on the one hand, neurons have a limited glycolytic capacity (4) and thus are particularly sensitive to the aging-associated decline in mitochondrial bioenergetics (5). On the other hand, intraneuronal accumulation of ubiquitinated proteins, indicative of proteasome malfunction, is a hallmark of most chronic neurodegenerative diseases including AD (6). Notably, the impact of mitochondrial impairment on proteasome function remains poorly defined.

One of the principal mechanisms by which mitochondrial dysfunction contributes to aging and neurodegeneration is via the limitation in ATP production that can cause an energy crisis in neurons (7). Brain glucose hypometabolism is detected early in AD patients and is implicated in the initiation and progression of AD pathology (8). ATP loss in AD brains was estimated

* This work was supported, in whole or in part, by National Institutes of Health Grants R01 AG028847 (to M. E. F.-P.) from the NIA and U54 NS041073 (Specialized Neuroscience Research Programs (SNRP)) (to M. E. F.-P., head of sub-project) from the NINDS.
[1] Both authors contributed equally to this work.
[2] To whom correspondence should be addressed: Dept. of Biological Sciences, Hunter College and Graduate Center, City University of New York, 695 Park Ave., New York, NY 10065. Tel.: 212-650-3565; Fax: 212-772-5227; E-mail: pereira@genectr.hunter.cuny.edu.

[3] The abbreviations used are: AD, Alzheimer disease; 6-CFDA, 6-carboxyfluorescein diacetate; H_2DCFDA, 5-(and-6)-carboxy-2′,7′-dichlorodihydrofluorescein diacetate; DMSO, dimethyl sulfoxide; MTT, 3-(4,5-dimethylthiazol-2-yl)-2,5-diphenyl tetrazolium bromide; PI, propidium iodide; ROS, reactive oxygen species; Rpn, regulatory particle non-ATPase; Rpt, regulatory particle triple-A ATPase; Suc-LLVY-AMC, succinyl-Leu-Leu-Val-Tyr-7-amino-4-methylcoumarin; TMRE, tetramethylrhodamine ethyl ester; Ub protein, ubiquitinated protein; UPP, ubiquitin/proteasome pathway; Cp3, calpain inhibitor III; Z, benzyloxycarbonyl; Nle, norleucine.

to reach as much as 50% in stable advanced dementia (9). This energy deficit may have a drastic impact on brain function. Degradation of proteins by the 26S proteasome is highly dependent on ATP binding and hydrolysis (10).

Another deleterious mechanism associated with mitochondrial dysfunction is a net increase in the production of reactive oxygen species (11). Oxidative stress induced by reactive oxygen species (ROS) alters the structure of cellular proteins (12), which, if not repaired, must be removed by proteolysis to prevent their accumulation and aggregation. One of the major roles of the proteasome is to degrade oxidatively modified proteins, but whether ubiquitination is required remains elusive (13). Some studies support the notion that oxidatively modified proteins in cells are removed by the 20S proteasome independently of ubiquitination (14). Others demonstrate that upon oxidative stress, there is an increase in the levels of ubiquitinated proteins and in ubiquitin-activating and ubiquitin-conjugating enzyme activities, suggesting that the ubiquitination machinery is recruited to degrade oxidatively modified proteins (15). This is an important issue because there is ample evidence that neural tissue is especially vulnerable to oxidative stress, which plays an important role in many neurodegenerative disorders (16). Neurons exhibit a higher sensitivity to proteasome inhibition than astrocytes, mostly because they undergo increased levels of oxidized proteins (17). Impaired clearance of oxidatively modified proteins can cause their aggregation and directly promote progression of the neurodegenerative process (18). Both deleterious consequences of mitochondrial impairment, *i.e.* restricted ATP-generating capacity and ROS production, are likely to contribute to impaired proteasome-dependent proteolysis in neurons (10, 19, 20).

It is postulated that in neurons, even a modest restriction of ATP production by mitochondria far outweighs the negligible effects of ROS, although the underlying mechanisms are not clearly understood (7). In our current study with neurons, we demonstrate that low ATP levels caused by mitochondrial dysfunction correlate with impairment of the ubiquitin/proteasome pathway (UPP); there is a decline in E1 and 26S proteasome activities, both of which are energy-dependent, with a concomitant rise in 20S proteasomes. This decline in UPP function occurs upon acute and long term mitochondrial impairment. Notably, upon energy depletion, calpain activation leads to the selective cleavage of Rpn10, a 26S proteasome subunit. Other proteasome subunits tested were not affected. Rpn10 cleavage, combined with ATP depletion, contributes to the demise of 26S proteasome function, a critical step in the UPP. We postulate that under acute mitochondrial stress conditions, unregulated and energy-independent protein degradation via 20S proteasomes could carry out the degradation of randomly unfolded oxidized proteins. However, regulated and ATP-dependent protein degradation via the UPP is essential for long term neuronal survival.

EXPERIMENTAL PROCEDURES

Materials—The following inhibitors were used: oligomycin A, antimycin A, rotenone, and chloroquine (Sigma-Aldrich); epoxomicin (Peptides International Inc.); calpain inhibitor III and calpeptin (Calbiochem/EMD Bioscience). The following substrate was used: Suc-LLVY-AMC (Bachem Bioscience Inc.). The following primary antibodies were used: rabbit polyclonal anti-ubiquitinated proteins (1:1500, catalog number Z0458, Dako North America); rabbit polyclonal anti-β5 (1:5000, catalog number PW8895), mouse monoclonal anti-Rpt6 (1:2000, catalog number PW9265), anti-Rpn10 (1:2000, catalog number PW9250), anti-α5 (1:2000, catalog number PW8125), anti-Rpn2 (1:2000, catalog number PW9270), and anti-Rpt5 (1:2000, catalog number PW8770), all from ENZO Life Sciences, Inc.; mouse monoclonal anti-β-actin (1:10,000, catalog number A-2228, Sigma); rabbit polyclonal anti-caspase 3 (1:1000, catalog number 9662), anti-UBE1a (1:1000, catalog number 4890), and anti-E2-25K/Hip2 (1:1000, catalog number 3847), all from Cell Signaling Technology; mouse monoclonal anti-spectrin α chain (1:5000, clone AA6, catalog number MAB1622, Millipore); mouse monoclonal anti-βIII-tubulin (1:10,000, catalog number MMS-435P, Covance); and mouse monoclonal Tau C5 (1:50,000; detects all Tau isoforms; epitope, residues 210–241), courtesy of Dr. L. Binder (Northwestern University, Chicago, IL). Secondary antibodies with HRP conjugate (1:10,000) were from Bio-Rad Laboratories.

Cell Cultures—Dissociated cultures from Sprague-Dawley rat embryonic (embryonic day 18, both sexes) cerebral cortical neurons were prepared as follows. The isolated cortices free of meninges were digested with papain (0.5 mg/ml from Worthington Biochemical) in Hibernate E without calcium (BrainBits LLC) at 37 °C for 30 min in a humidified atmosphere containing 5% CO_2. After removal of the enzymatic solution, the tissues were gently dissociated in Neurobasal medium (Invitrogen). Dissociated tissues were centrifuged at 300 $\times$ *g* for 2 min. The pellet was resuspended in Neurobasal medium without antibiotics and plated on 10-cm dishes precoated with 50 μg/ml poly-D-lysine (Sigma). Cells were plated at a density of 6×10^6 cells/10-cm dish, or 2.5×10^5 cells/well on 24-well plates (cell viability only). Cultures were maintained in Neurobasal medium supplemented with 2% B27 and 0.5 mM L-GlutaMAX (all from Invitrogen) at 37 °C in a humidified atmosphere containing 5% CO_2. Half of the medium was changed every 4 days. Experiments were run upon 8–11 days *in vitro*. According to the manufacturer's specifications, Neurobasal medium contains several proprietary factors that ensure a mostly pure (>95%) neuronal culture; glial growth is inhibited without a need for the anti-mitotic agent arabinofuranosyl cytidine (21, 22).

Culture Treatments—Cortical neurons were treated acutely (1.5, 2, 4, 8, or 16 h) with DMSO or with the different drugs in DMSO added directly to DMEM without serum, supplemented with 0.5 mM L-GlutaMAX and 1 mM sodium pyruvate (all from Invitrogen). The final DMSO concentration in the medium was 0.5%. For long term (1 day to 7 days) studies, neurons were maintained for the entire time in DMEM with 2% B27 supplemented with 0.5 mM L-GlutaMAX and 1 mM sodium pyruvate. Drugs were added once at the beginning of each experiment, following the same protocol as for the acute studies.

ATP Assay—Steady state ATP content was measured with a kit using the sensitive luciferin/luciferase system (Molecular Probes). This assay is based on luciferase requiring ATP for light production using luciferin as a substrate. Cells were har-

vested with 4% trichloroacetic acid followed by centrifugation (19,000 × *g*, 15 min at 4 °C). ATP steady state levels were determined in cleared supernatants upon neutralizing the samples with 10 mM Tris-HCl, pH 8.0. Samples were then added to the reaction buffer containing luciferin and assayed using a Luminoskan Ascent microplate luminometer (Thermo Electron). Protein concentration was determined with the bicinchoninic acid assay (BCA) kit (Pierce) upon resuspending the pellet with buffer (10 mM Tris-HCl, pH 8.0 and 1% SDS), and sonication. ATP levels were normalized for protein concentration.

Mitochondrial Membrane Potential and ROS Measurements—Upon treatment with the drugs, mitochondrial membrane potential ($\Delta\Psi_m$) was assessed with TMRE (Abcam Inc.), and ROS was assessed with H_2DCFDA (Invitrogen). At the designated time points, treatment medium (DMEM) with the drugs was removed, and fresh DMEM without drugs but with TMRE (200 nM) or H_2DCFDA (20 μM) was added to separate cultures. Following a 30-min dye-loading incubation that included Hoechst 33342 (2′-[4-ethoxyphenyl]-5-[4-methyl-1-piperazinyl]-2,5′-bi-1*H*-benzimidazole trihydrochloride trihydrate) for nuclear staining for the last 5 min, the cultures were changed to fresh dye-free DMEM. The dyes were allowed to re-equilibrate in the fresh dye-free medium, and then TMRE and H_2DCFDA fluorescence was imaged on a Nikon Eclipse TE 200 inverted epifluorescence microscope. The following excitation/emission wavelengths were used: for TMRE (red), 549/575 nm; for ROS (green), 495/529 nm; and for Hoechst 33342 (blue), 350/461 nm. For each condition, total fluorescence from cells was semiquantified in each image field using ImageJ, typically for 10–15 images per group pooled over two independent experiments for each group, and normalized to time-matched DMSO (vehicle) control = 1. Images with effectively no signal were excluded from analysis (using ImageJ from the National Institutes of Health).

Cell Viability Assays—Cell viability was assessed with the 3-(4,5-dimethylthiazol-2-yl)-2,5-diphenyl tetrazolium bromide (MTT) assay as described in Ref. 23. In addition, propidium iodide cell staining (Invitrogen) and 6-carboxyfluorescein diacetate (6-CFDA) (Sigma) cell staining were carried out following the respective manufacturer's specifications.

Western Blotting—After treatment, cells were rinsed twice with PBS and harvested by gently scraping into hot (100 °C) SDS buffer (0.01 M Tris-EDTA, pH 7.5, and 1% SDS) to make sure all intracellular proteins were included. Samples were subjected to a 5-min boil at 100 °C followed by brief sonication. After determination of the protein concentration with the BCA kit, the following was added to each sample (final concentrations): β-mercaptoethanol (4%), bromphenol blue (0.005%), and glycerol (4%). Following SDS-PAGE on 6, 8, 10, or 12% polyacrylamide gels, proteins were transferred to an Immobilon-P membrane (Millipore). The membranes were probed with the respective antibodies, and antigens were visualized by a standard chemiluminescent horseradish peroxidase method with the ECL reagent. Semiquantification of protein detection was done by image analysis with ImageJ.

Evaluation of Endogenous E1- and E2-25k-Ubiquitin Thiol Esters—Upon treatment with vehicle (control, DMSO) or with the respective drugs, cortical neurons were washed twice with PBS, harvested with a thiol-stabilizing buffer (5 mM Tris-HCl, pH 7.8, 8.7 M urea, 1% Nonidet P-40, 20 mM *N*-ethylmaleimide, 3 mM EDTA, 2% protease inhibitor mixture (Sigma)), and kept on ice for 15 min for lysing, as described in Ref. 24. Samples were sonicated for 10 s, centrifuged at 19,000 × *g* for 15 min at 4 °C, mixed (30 μg) at 1:2 volume with thiol ester gel buffer (33 mM Tris-HCl, pH 6.8, 2.7 M urea, 2.5% SDS, and 13% glycerol), and boiled for 5 min. After determination of the protein concentration with the Bradford assay (Bio-Rad Laboratories), the normalized samples were separated into reducing (with 4% β-mercaptoethanol) and nonreducing (no β-mercaptoethanol) aliquots for SDS-PAGE followed by Western blotting with anti-E1 and anti-E2 antibodies, as described above.

In-gel Proteasome Activity and Proteasome Levels—Upon treatment with vehicle (control, DMSO) or the respective drugs, cells were washed twice with PBS and harvested for the in-gel assay as described in Ref. 25. The native gels loaded with 30 μg of protein/lane were run at 150 V for 120 min. The in-gel proteasome activity was detected by incubating the native gel on a rocker for 10 min at 37 °C with 15 ml of 300 μM Suc-LLVY-AMC followed by exposure to UV light (360 nm). Gels were photographed with a NIKON COOLPIX 8700 camera with a 3-4219 fluorescent green filter (Peca Products, Inc.). Proteins on the native gels were transferred (110 mA) for 2 h onto PVDF membranes. Immunoblotting was carried out for detection of the 20S and 26S proteasomes with the anti-Rpt6 and anti-β5 antibodies, which react with subunits of the 19S or the 20S particles, respectively, thus detecting 26S and 20S fully assembled proteasomes. Antigens were visualized by a chemiluminescent horseradish peroxidase method with the ECL reagent. The values in the tables shown in Figs. 3 and 4 reflect the semiquantification obtained with the Rpt6 antibody for 26S proteasome levels (single and double capped) as it generated the strongest signal and with the β5 antibody for 20S proteasome levels.

Glycerol Density Gradient Centrifugation—Cells were harvested in 25 mM Tris-HCl, pH 7.5, 2 mM ATP, and 1 mM DTT. Following homogenization and sonication, the lysates were centrifuged (19,000 × *g* for 15 min) at 4 °C. The cleared supernatants (1 mg of protein/sample) were subjected to centrifugation (83,000 × *g* for 24 h) at 4 °C in a Beckman SW41 rotor in a 10–40% glycerol gradient (fractions 1–24) made in the same lysis buffer. Following centrifugation, 24 fractions (500 μl each) were collected. Aliquots (50 μl) of each fraction were assayed for chymotrypsin-like activity with the substrate Suc-LLVY-AMC after 3-h incubations at 37 °C as described in Ref. 26 and using a Gemini EM spectrofluorometer (Molecular Devices). Proteins were precipitated with acetone from 450 μl of each fraction and subjected to Western blot analysis (10% gels). The membranes were probed with the respective antibodies, and antigens were visualized by a standard chemiluminescent horseradish peroxidase method with the ECL reagent.

Statistical Analysis—Statistical significance was estimated using one-way analysis of variance (Tukey-Kramer multiple comparison test) or Student's *t* test with Welch's correction (Fig. 2 only) with the Prism 5 program (GraphPad Software).

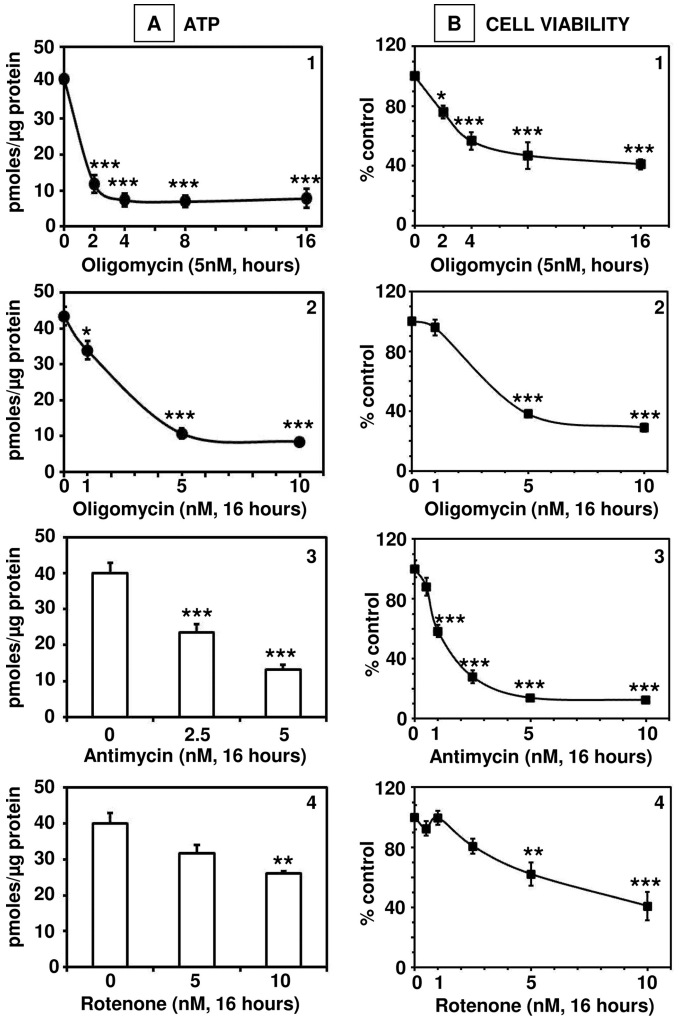

FIGURE 1. **Effects of oligomycin, antimycin and rotenone on ATP levels and viability in rat cerebral cortical neurons.** Neurons were treated with oligomycin (*panels 1* and *2*), antimycin (*panels 3*), and rotenone (*panels 4*) for the times and concentrations indicated. *A*, ATP steady state levels (pmol/μg of protein) were assessed with the luciferin/luciferase system. *B*, cell viability was assessed with the MTT assay. The percentages represent the ratio between the data for each condition and control (100%). Values indicate means and S.E. from at least three experiments per group. *Asterisks* identify values that are significantly different from control (*, $p < 0.05$; **, $p < 0.01$; ***, $p < 0.001$).

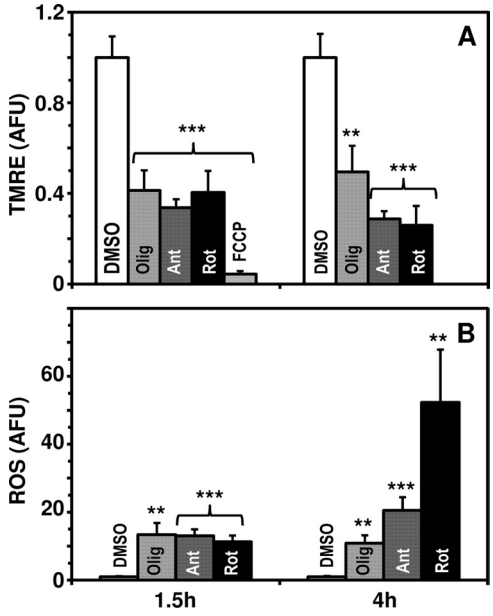

FIGURE 2. **Effects of oligomycin (*Olig*), antimycin (*Ant*), and rotenone (*Rot*) on mitochondrial membrane potential $\Delta\Psi_m$ and ROS in rat cerebral cortical neurons.** Neurons were treated with oligomycin (5 nM), antimycin (5 nM), and rotenone (10 nM) for the times indicated. *A*, $\Delta\Psi_m$ was assessed with TMRE. The effect of the uncoupler carbonyl cyanide *p*-trifluoromethoxyphenylhydrazone (*FCCP*) is shown for comparison. *AFU*, arbitrary fluorescent units. *B*, ROS was assessed with H_2DCFDA. Total fluorescence from cells was quantified in each image field using ImageJ. Values (arbitrary fluorescent units (*AFU*)) indicate means and S.E. from 10–15 images per group pooled over two independent experiments for each group and normalized to time-matched DMSO (vehicle) control = 1. *Asterisks* identify values that are significantly different from control (**, $p < 0.01$; ***, $p < 0.001$).

RESULTS

Oligomycin, Antimycin, and Rotenone as Mitochondrial Inhibitors—To investigate the link between mitochondrial impairment and loss of neuronal viability, rat cerebral cortical neurons were treated with three mitochondrial inhibitors that affect different elements of the electron transport chain. 1) Rotenone binds to ND1 and inhibits NADH-ubiquinone reductase activity of complex I (27); 2) antimycin A binds to the quinone reduction site of complex III (ubiquinol-cytochrome *c* oxidoreductase), inhibiting the reduction of cytochrome *c* (28); and 3) oligomycin binds to a polypeptide in the F_0 baseplate and blocks ATP synthesis by the F_0/F_1 mitochondrial ATP synthase (29). As shown in Fig. 1*A*, all three drugs decrease ATP levels in a concentration-dependent manner. Oligomycin was the most efficient, as 5 nM of this drug lowered ATP levels by ~75%. The 25% ATP that remains upon oligomycin treatment must be generated in a mitochondria-independent manner by glycolysis. The decline in ATP levels induced a loss of neuronal viability (Fig. 1*B*) assessed with the MTT assay, which is reduced largely within the cytoplasm of most cells (30, 31). From the three drugs tested, rotenone caused the weakest changes in all assays, except for ROS.

Effect of Oligomycin, Antimycin, and Rotenone on $\Delta\Psi_m$ and ROS—Oligomycin (5 nM), antimycin (5 nM), and rotenone (10 nM) all decreased TMRE signal after 1.5- or 4-h treatment, as did the protonophore carbonyl cyanide *p*-trifluoromethoxyphenylhydrazone (100 nM) (Fig. 2*A*). This decline in TMRE signal is likely to reflect a decrease in $\Delta\Psi_m$. By inhibiting complex I and III, respectively, and thus reducing proton efflux from the mitochondria, rotenone and antimycin are classically associated with decreased $\Delta\Psi_m$, as supported by the decline in TMRE signal. Under nonglycolytic conditions, acute oligomycin treatment is typically associated with increased $\Delta\Psi_m$ due to the oligomycin-induced blockade of proton influx through the ATP synthase. Oligomycin will decrease $\Delta\Psi_m$ when $\Delta\Psi_m$ is being maintained by reversal of the ATP synthase by hydrolyzing glycolysis-derived ATP (32), but this scenario is not consistent with the oligomycin-induced decline in ATP levels at these same 1.5- and 4-h time points (Fig. 1). Rather, a decline in $\Delta\Psi_m$ caused by longer term oligomycin treatment would be consistent with the overall loss of metabolic (*i.e.* namely NADH) activity we observed by MTT assay at these same time points, and may also be caused by uncoupling proteins activated in response to prolonged elevation of $\Delta\Psi_m$ (33, 34).

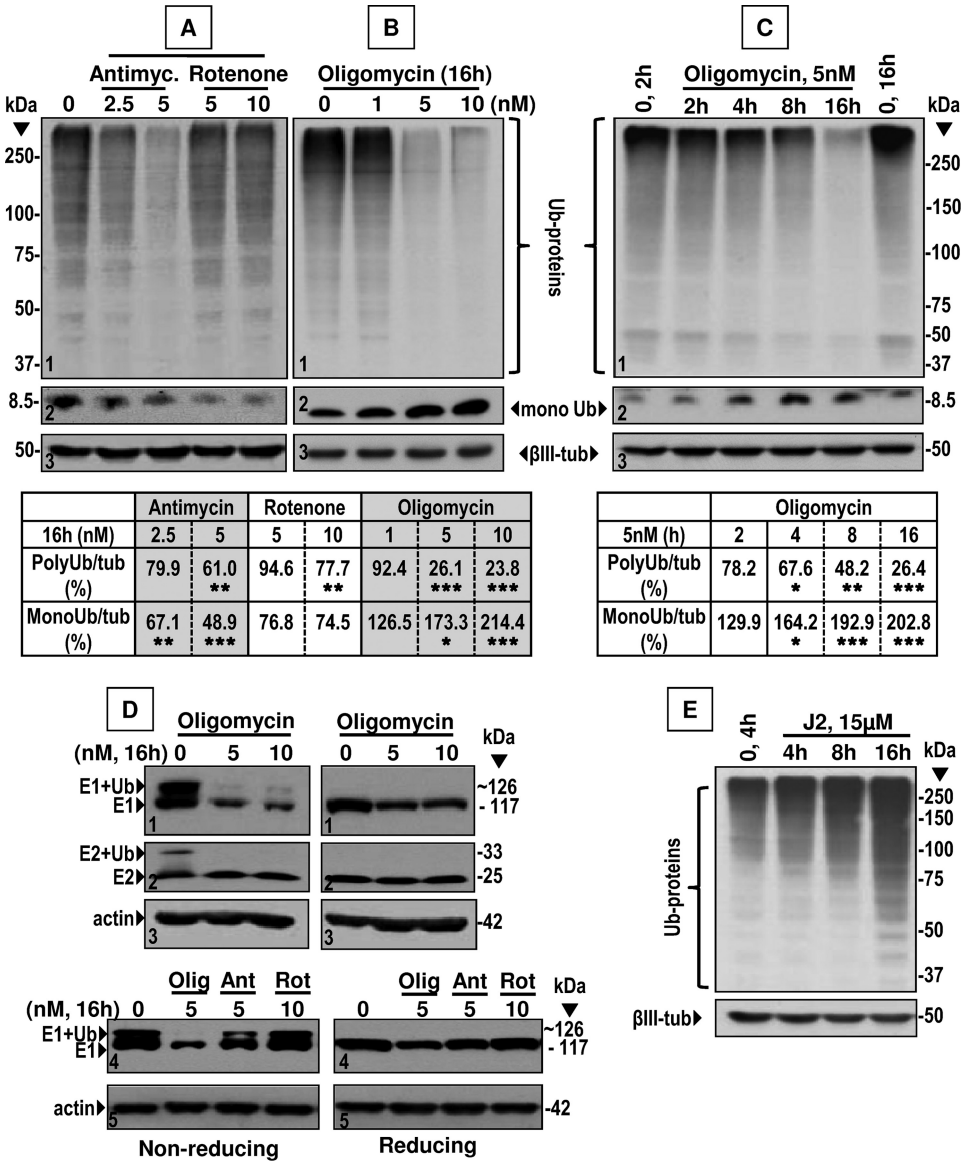

FIGURE 3. **Effects of oligomycin, antimycin (*Antimyc.*), and rotenone on Ub proteins, monoubiquitin (*MonoUb*), and E1- and E2-ubiquitin thiol esters in rat cerebral cortical neurons.** Neurons were treated as indicated. Total lysates were analyzed by Western blotting (30 μg of protein/lane) probed with the respective antibodies for detection of proteins as follows. *A–C*, Ub proteins (*panels 1*), free monoubiquitin (*panels 2*), and βIII-tubulin (*βIII-tub*, loading control, *panels 3*). *D*, E1-ubiquitin (*E1+Ub*) and E2-ubiquitin (*E2+Ub*) thiol esters (*upper bands*) and native E1 and E2 (*lower bands*) run under nonreducing conditions (*left panels*) or reducing conditions with β-mercaptoethanol (*right panels*); actin (loading control) was detected in *panels 3* and *5*. *Olig*, oligomycin; *Ant*, antimycin; *Rot*, rotenone. *E*, effect of prostaglandin J_2 (15 μM; *J2*) on Ub proteins and βIII-tubulin (*βIII-tub*, loading control). Molecular mass markers in kDa are shown on the *left* and *right*. In *A–C*, the levels of ubiquitinated proteins (*polyUb/βIII-tub*) and free monoubiquitin (*monoUb/βIII-tub*) were semiquantified by densitometry (*values in tables*). Data represent the percentage of the pixel ratio for Ub proteins and free monoubiquitin over the respective loading control for each condition when compared with control (DMSO, 100%). Values are means from at least three experiments. *Asterisks* identify values that are significantly different from control (*, $p < 0.05$, **, $p < 0.01$, ***, $p < 0.001$).

ROS are generated whenever electron transport through the electron transport chain is slowed (29, 35). As expected, ROS production in response to 1.5 or 4 h of oligomycin (5 nM), antimycin (5 nM), and rotenone (10 nM) treatment was elevated as measured by H_2DCFDA fluorescence (Fig. 2*B*). For the TMRE and ROS measurements, only the 1.5- and 4-h time points were quantified because quantification of later time points would be confounded by significant loss of cell integrity and thus not informative.

The Decline in Polyubiquitinated Proteins Induced by the Three Mitochondrial Inhibitors Is Linked to E1 Failure—Chronic neurodegenerative disorders such as AD are linked to mitochondrial dysfunction and to accumulation/aggregation of ubiquitinated (Ub) proteins (37). We examined the effect of the three mitochondrial inhibitors on Ub protein levels in the cortical neurons. Oligomycin and antimycin decreased Ub proteins in a concentration- (Fig. 3, *A* and *B*, *panel 1*) and time-dependent (established for oligomycin, Fig. 3*C*, *panel 1*) manner. Only the highest concentration of rotenone tested (10 nM) significantly lowered Ub protein levels. In neurons treated with oligomycin, but not with antimycin or rotenone, the decline in Ub proteins coincided with a rise in free monoubiquitin, observed in a concentration- (Fig. 3*B*, *panel 2*) and time-dependent (Fig. 3*C*, *panel 2*) manner. The effect of prostaglandin J_2 on

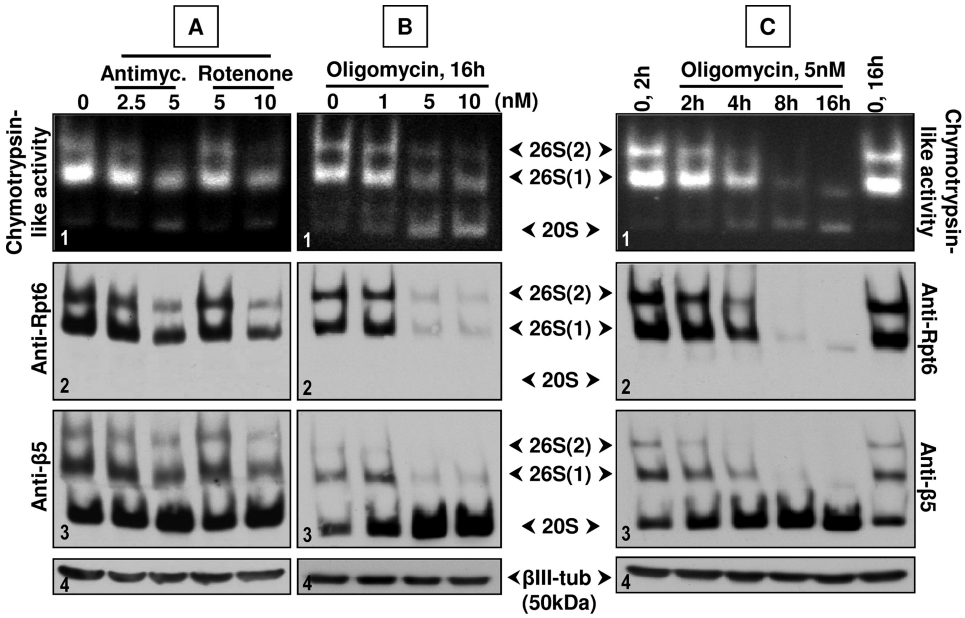

Proteasome activity

	Antimycin		Rotenone		Oligomycin		
16h (nM)	2.5	5	5	10	1	5	10
26S (2) (%)	64.5 ***	17.8 ***	74.3	42.1 **	87.2	20.6 ***	14.5 ***
26S (1) (%)	99.8	57.3 **	80.4	57.8 *	104.6	49.5 **	43.3 **
20S (%)	184.5	237.6 *	95.1	103.9	179.6	290.0 **	298.3 **

	Oligomycin			
5nM (h)	2	4	8	16
26S (2) (%)	87.4	57.7 **	16.4 ***	19.2 ***
26S (1) (%)	90.0	76.1	34.4 ***	43.8 **
20S (%)	146.4	225.4	357.5 ***	279.4 *

Proteasome levels

	Antimycin		Rotenone		Oligomycin		
16h (nM)	2.5	5	5	10	1	5	10
26S (2) (%)	63.2 *	13.2 ***	80.5	43.5 *	99.7	6.38 ***	5.11 ***
26S (1) (%)	100.4	63.6 *	93.6	74.1 **	118.6	25.1 ***	15.0 ***
20S (%)	137.2 *	165.3 ***	87.3	120.0	152.2	266.6 ***	290.8 ***

	Oligomycin			
5nM (h)	2	4	8	16
26S (2) (%)	84.9	63.0 ***	5.7 ***	3.3 ***
26S (1) (%)	89.6	76.2	23.6 ***	43.9 **
20S (%)	119.2	181.6	258.4 **	286.8 ***

FIGURE 4. **Effects of oligomycin, antimycin and rotenone on proteasome activity and levels in rat cerebral cortical neurons.** *A–C*, neurons were treated for 16 h with antimycin (*Antimyc.*) or rotenone (*A*) or oligomycin (*B*) or with 5 nM oligomycin for different time points (*C*). Cleared lysates (30 μg/sample) were subjected to nondenaturing gel electrophoresis as described under "Experimental Procedures." Fully assembled 26S and 20S proteasomal (indicated in the *middle* by *arrows*) chymotrypsin-like activity was assessed with Suc-LLVY-AMC by the in-gel assay (*panels 1*). Proteasome levels were detected by immunoblotting with anti-Rpt6 (*panels 2*) and anti-β5 antibodies (*panels 3*). Proteasome chymotrypsin-like activity and levels were semiquantified by densitometry (*values in tables*). The percentages represent the ratio between data for each condition and control (DMSO) considered to be 100%. Values are means from at least three experiments. *Asterisks* identify values that are significantly different from control (*, $p < 0.05$, **, $p < 0.01$, ***, $p < 0.001$).

Ub proteins in neurons is shown for comparison in Fig. 3*E*. Prostaglandin J_2 is an endogenous product of inflammation (38) shown to increase the levels of Ub proteins (39), in contrast to the mitochondria toxins.

To address a mechanism mediating the decline in Ub proteins induced by oligomycin, we focused on the E1A ubiquitin-activating enzyme and on the E2-conjugating enzyme E2-25K. E1 activity requires ATP for formation of a thiol ester adduct with ubiquitin, a process that is sensitive to reducing agents, such as β-mercaptoethanol (40). In principle, if E1 activity is impaired, all protein ubiquitination, including E1-E2 transthiolation, should be diminished. To assess E1- and E2-ubiquitin thiol ester levels, the samples were run on SDS-PAGE under reducing (with β-mercaptoethanol) and nonreducing (without β-mercaptoethanol) conditions. As shown in Fig. 3*D* (*panels 1* and *4*, *left lanes*), under nonreducing conditions, E1-ubiquitin thiol ester (~126 kDa) migrated ~9 kDa above native E1 (117 kDa), consistent with the additional mass of ubiquitin. Oligomycin and antimycin treatment abolished the E1-ubiquitin thiol ester, reflecting the loss of the ubiquitin monomer. The effect of rotenone on E1-ubiquitin thiol ester was very minor (undetectable). A similar pattern was observed for the E2-conjugating enzyme E2-25K. Its E2-ubiquitin thiol ester (~33 kDa), which is dependent on E1 transthiolation activity, was eliminated in neurons treated with oligomycin (Fig. 3*D*, *panel 2*, *three left lanes*). Under reducing conditions (*panels 1*, *2*, and *4*, *right lanes*), only native E1 and E2 were detected. Together, these data demonstrate that due to mitochondrial impairment, ATP depletion in neurons prevents E1 from forming thiol ester intermediates with ubiquitin, resulting in an overall down-regulation of Ub proteins.

Perturbing Mitochondria in Neurons Causes a Decline in 26S Proteasomes and a Concomitant Increase in 20S Proteasomes—The activity and assembly of 26S proteasomes are highly dependent on ATP binding and hydrolysis (10, 41). We thus assessed, with the native in-gel assay, the effects of the three mitochondrial inhibitors on proteasome activity and levels in the cortical neurons. The in-gel assay detects the three assem-

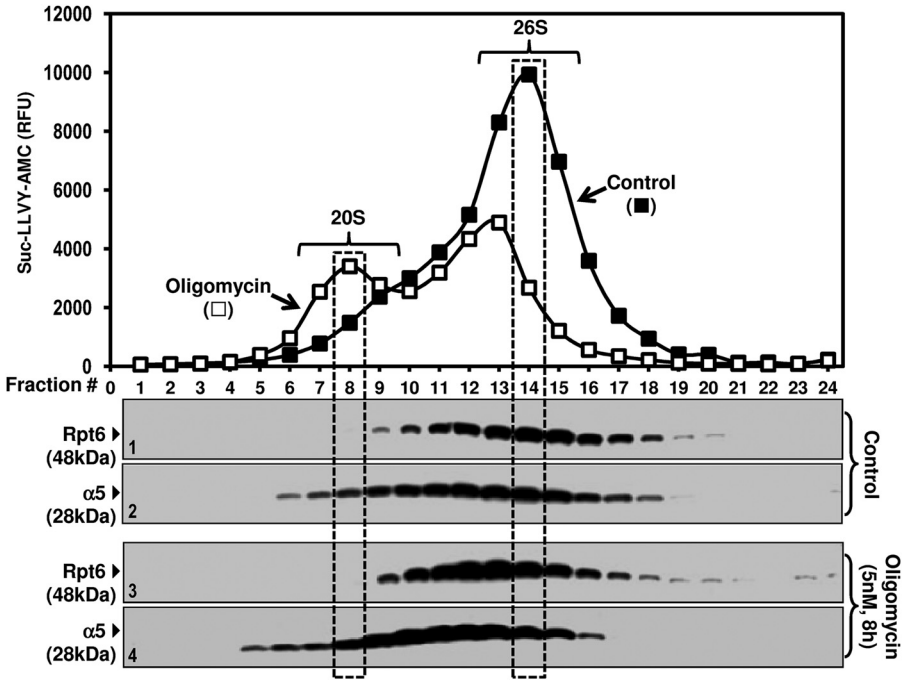

FIGURE 5. **Effects of oligomycin on the sedimentation velocity of proteasomes in rat cerebral cortical neurons.** Total lysates (one mg protein/sample) were fractionated by glycerol density gradient centrifugation (10–40% glycerol corresponding to fractions 1–24). Aliquots (50 μl) of each fraction obtained from control- (*black squares*) and oligomycin- (5 nM, 8 h, *white squares*) treated cells were assayed for chymotrypsin-like activity with Suc-LLVY-AMC (graph). Immunoblot analyses of each fraction probed with antibodies that react with Rpt6 (19S regulatory particle, *panels 1* and *3*) or α5, (core particle, *panels 2* and *4*) are shown. Proteins were precipitated with acetone from 450 μl of each fraction. Similar results were obtained in triplicate experiments. *RFU*, relative fluorescent units.

bled forms of the proteasome: 26S proteasomes with either two regulatory caps (26S(2)) or one cap (26S(1)) and the 20S core particle alone (20S). Proteasome activity was determined with the substrate Suc-LLVY-AMC, which assesses the chymotrypsin-like activity (Fig. 4, *A*–C, *panel 1*). Under control conditions (*lanes marked with 0*), the activity of the 20S proteasome is substantially lower than that of the 26S because the 20S is a latent proteasome form (42). Proteasome levels were determined by immunoblotting with the anti-Rpt6 antibody that reacts with an ATPase subunit of the 19S particle (Fig. 4, *A*–C, *panel 2*) and with the anti-β5 antibody (Fig. 4, *A*–C, *panel 3*). The β5 subunit is a component of the 20S core; thus, its antibody detects assembled 26S and 20S proteasomes. The three mitochondria inhibitors decreased 26S proteasome activity in a concentration- (Fig. 4, *A* and *B*, *panel 1*) and time-dependent (oligomycin, Fig. 4*C*, *panel 1*) manner. Furthermore, the three drugs caused the disassembly of the 26S proteasome as its levels decreased, whereas the levels of the 20S proteasome increased (Fig. 4, *A*–C, *panels 2* and *3*). Semiquantification of proteasome activity and levels for each condition is listed in the respective tables shown in Fig. 4.

We corroborated by glycerol gradient fractionation that mitochondrial dysfunction in neurons causes a shift from 26S to 20S proteasomes (Fig. 5). Because oligomycin has the strongest effect, we only tested this drug here. Total extracts from cells treated with vehicle (DMSO, control) or oligomycin (5 nM, 8 h) were fractionated by glycerol density gradient centrifugation. Fractions were analyzed for Suc-LLVY-AMC hydrolysis, which reflects the chymotrypsin-like activity (graph). When compared with control, the chymotrypsin-like activity of oligomycin-treated cells was significantly reduced in the fractions corresponding to the elution of the 26S proteasomes: fractions 12–16 (*peak for 26S*), compare oligomycin treatment (*white squares*) with control (*black squares*). In contrast, the activity of 20S proteasomes (fractions 7–9, *peak for 20S*) was increased in the oligomycin-treated cells.

To confirm the proteasome elution pattern, aliquots from each fraction were subjected to Western blot analyses with the anti-Rpt6 antibody that reacts with an ATPase subunit of the 19S particle (*rows 1* and *3*, control- and oligomycin-treated, respectively) and the anti-α5 antibody that reacts with a subunit of the 20S core particle, (*rows 2* and *4*, control- and oligomycin-treated, respectively). From these experiments, we can conclude that an 8-h treatment with 5 nM oligomycin triggers the disassembly of 26S proteasomes with a parallel increase in 20S proteasomes.

Mitochondrial Dysfunction Causes a Selective Decline in the Levels of the Rpn10 Subunit of the 19S Particle That Concurs with Calpain but Not Caspase Activation—We considered that the decrease in 26S proteasome levels induced by oligomycin could be caused by a reduction in subunit levels. We thus investigated the effect of oligomycin on subunits of the 19S (Rpn2, Rpt5, Rpt6, and Rpn10) and 20S (α5 and β5) proteasome particles. Notably, from all of the proteasome subunits tested, only Rpn10 levels were reduced by oligomycin in a concentration- (Fig. 6*A*, *top row*) and time-dependent (Fig. 6*B*, *top row*) manner.

Because oligomycin triggers a loss of neuronal viability, we contemplated the possibility that apoptosis was induced and that the ensuing caspase activation was responsible for cleaving

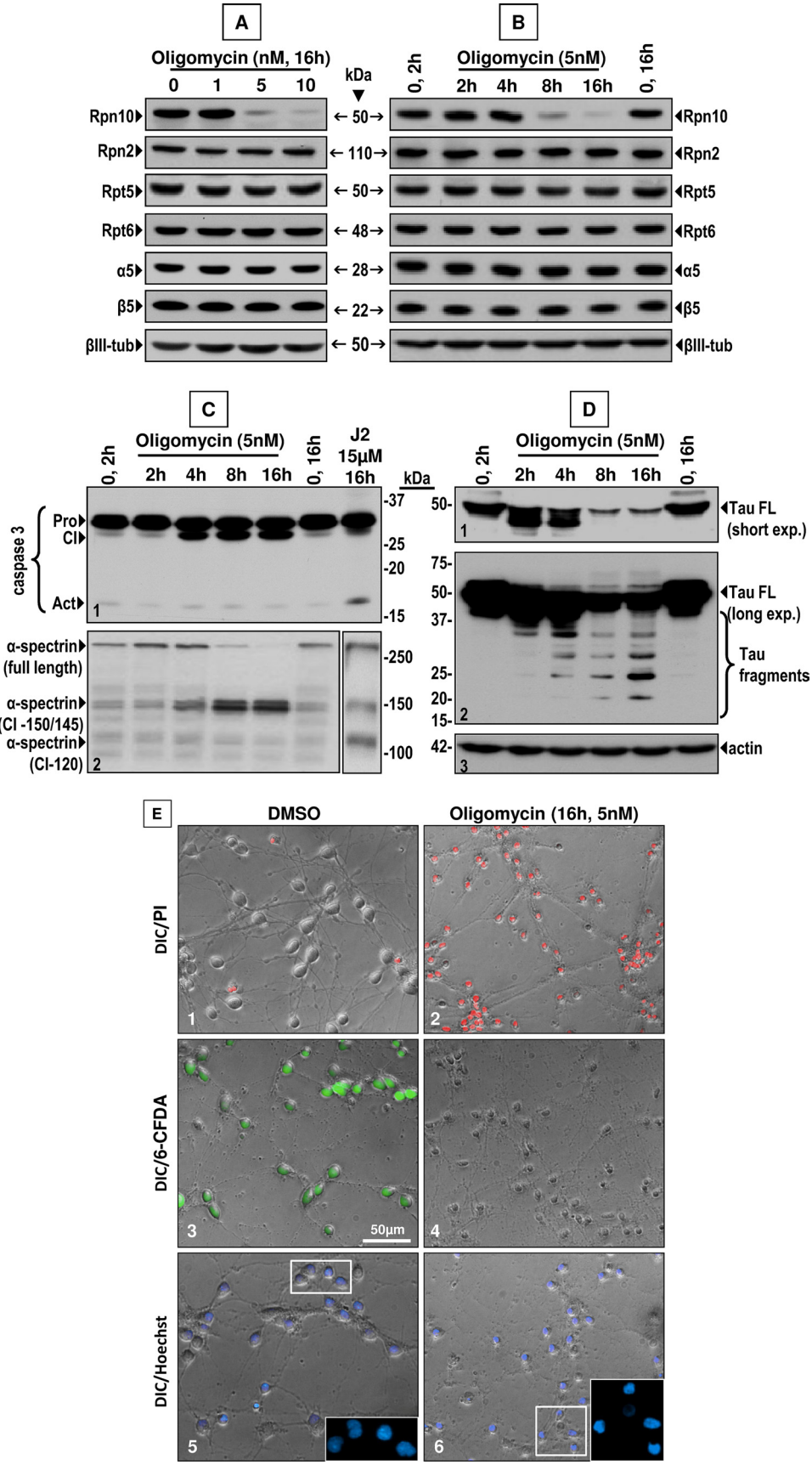
A
Oligomycin (nM, 16h)
0 1 5 10
kDa
Rpn10
Rpn2
Rpt5
Rpt6
α5
β5
βIII-tub
← 50→
← 110→
← 50→
← 48→
← 28→
← 22→
← 50→
B
0, 2h
Oligomycin (5nM)
2h 4h 8h 16h
0, 16h
C
J2 15μM 16h
caspase 3
Pro
Cl
Act
α-spectrin (full length)
α-spectrin (Cl -150/145)
α-spectrin (Cl-120)
-37
-25
-20
-15
-250
-150
-100
D
Tau FL (short exp.)
Tau FL (long exp.)
Tau fragments
actin
50-
75-
37-
25-
20-
15-
42-
E
DMSO
Oligomycin (16h, 5nM)
DIC/PI
DIC/6-CFDA
DIC/Hoechst
50μm

Rpn10, thus decreasing its levels. However, we did not observe cleavage of pro-caspase 3 (33 kDa) to its active form (17 kDa) in neurons treated with oligomycin (Fig. 6*C*, *panel 1*). Instead, pro-caspase 3 was processed to an ~29-kDa fragment (Cl-caspase 3) and not to its active 17-kDa form. The latter 17-kDa fragment triggered by the endogenous product of inflammation prostaglandin J_2 is shown for comparison in Fig. 6*C* (*panel 1*, *last lane*). Prostaglandin J_2 is known to induce apoptosis in neurons (43).

We next investigated whether calpain was activated upon mitochondrial dysfunction by assessing cleavage of one of its substrates, α-spectrin. Oligomycin treatment clearly induced cleavage of α-spectrin (280 kDa) to 145/150-kDa fragments, which are indicative of calpain activation (Fig. 6*C*, *panel 2*). In contrast, there was no detection of the 120-kDa α-spectrin fragment, a marker of apoptotic cell death generated by caspase 3 processing of α-spectrin (44). For comparison, prostaglandin J_2-induced cleavage of α-spectrin to the caspase-mediated 120-kDa fragment is shown (Fig. 6*C*, *panel 2*, *last lane*). Oligomycin also induced the cleavage of another calpain substrate, the microtubule-associated protein Tau (Fig. 6*D*, *panels 1* and *2*). Tau is a major component of neurofibrillary tangles in AD (45). Together, these results suggest that the selective decline in Rpn10 induced by mitochondrial dysfunction may be triggered by calpain-mediated processing.

Fluorescence staining confirmed that oligomycin induces necrosis. Propidium iodide (PI) staining of oligomycin-treated neuronal cultures (Fig. 6*E*, *panel 2*) indicates necrotic cell death because due to the extensive membrane damage, PI quickly moves into necrotic cells. The intact membrane of living cells (Fig. 6*E*, *panel 1*) and apoptotic cells prevents PI cell entry (46). Although apoptosis affects mainly the nucleus, in its later phases, the plasma membrane becomes leaky and can also uptake PI (46). Staining with 6-CFDA is used to detect living cells. When this nonfluorescent compound enters living cells, it is hydrolyzed by esterases, generating 6-carboxyfluorescein that appears as green fluorescence (47). Thus, necrotic cells do not appear green (Fig. 6*E*, *panel 4*), whereas living cells do (Fig. 6*E*, *panel 3*). Nuclear morphology is shown with Hoechst staining (Fig. 6*E*, *panels 5* and *6*).

We established that antimycin mimics the effects of oligomycin on Rpn10, caspase 3, α-spectrin, and Tau cleavage (Fig. 7). However, rotenone had only weak or undetectable effects on the cleavage of the latter proteins (Fig. 7). Because Rpn11, a deubiquitinating subunit, is linked to mitochondrial function (48), we investigated whether its levels were altered by any of the three mitochondrial inhibitors. As shown in Fig. 7 (*panel 2*), no changes in Rpn11 were detected.

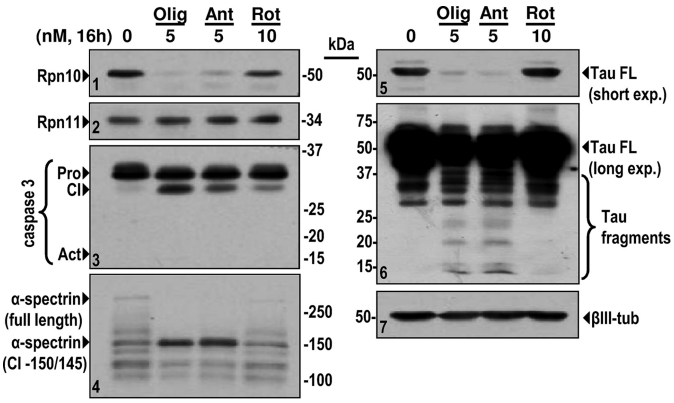

FIGURE 7. **Effects of antimycin and rotenone on Rpn10 (*panel 1*), Rpn11 (*panel 2*), caspase 3 (*panel 3*), α-spectrin (*panel 4*), and Tau cleavage (*panels 5 and 6*) in rat cerebral cortical neurons.** Neurons were treated for 16 h with antimycin (*Ant*) or rotenone (*Rot*). Oligomycin (*Olig*) was included for comparison. Total lysates were analyzed by Western blotting (30 μg of protein/lane) probed with the respective antibodies. *βIII-tub* indicates βIII-tubulin (used as loading control). Molecular mass markers in kDa are shown in the *center*. Similar data were obtained in triplicate experiments. The abbreviations indicate: *Pro* (full-length), *Cl* (cleaved), and *Act* (active) caspase 3; *Tau FL*, full-length Tau; *short exp.*, short exposure; *long exp.*, long exposure.

Upon Mitochondrial Impairment, Rpn10 Is Processed by Calpain and Not by Proteasomes or Lysosomes—Because oligomycin has the strongest effect, we only focused on this drug here. To sort out which proteolytic activity processes Rpn10 upon treatment with oligomycin, we pretreated neurons with inhibitors of the proteasome (epoxomicin), lysosome (chloroquine), and calpain (calpain inhibitor III (Cp3, Z-Val-Phe-CHO) and calpeptin (Z-Leu-Nle-CHO)). Only the calpain inhibitors (Fig. 8*A*, *dashed box*) prevented the decline in Rpn10 (*panel 1*). Furthermore, the calpain inhibitors blocked cleavage of pro-caspase 3 (*panel 2*), α-spectrin (*panel 3*), and Tau (*panel 4*). Pretreatment with the calpain inhibitors also prevented the decline in 26S proteasome activity (Fig. 8*B*, *panel 1*) and assembly (Fig. 8*B*, *panels 2* and *3*) triggered by oligomycin. Surprisingly, Cp3 by itself inhibited 26S proteasome activity without triggering its disassembly, whereas calpeptin stimulated the 20S proteasome. The two inhibitors *per se* did not alter proteasome levels by much; thus, their individual effects on proteasome activity could be due to a secondary effect on the proteasome itself (for Cp3) and/or on a putative 20S proteasome-activating factor regulated by calpain. Anyway, it is clear that the two calpain inhibitors prevented the negative effect of oligomycin on proteasomes.

The calpain inhibitors failed to prevent the decline in E1 activity (Fig. 8*C*) or the loss in viability induced by oligomycin (Fig. 8*D*). This is not surprising because the calpain inhibitors target calpain, but not ATP depletion.

FIGURE 6. **Effects of oligomycin on proteasome subunit levels, caspase 3, α-spectrin, and Tau cleavage in rat cerebral cortical neurons.** Neurons were treated as indicated. Total lysates were analyzed by Western blotting (30 μg of protein/lane) probed with the respective antibodies for detection of proteins as follows. *A* and *B*, proteasome subunits (19S particle, Rpn10, Rpn2, Rpt5, and Rpt6; 20S core, α5 and β5) and βIII-tubulin (*βIII-tub*, loading control). *C*, caspase 3 (*panel 1*) and α-spectrin (*panel 2*), with the effect of prostaglandin J_2 (*J2*) shown for comparison. *D*, Tau (*panels 1* and *2*) and actin (loading control, *panel 3*). Molecular mass markers in kDa are shown in the *center* (*A* and *B*), on the *right* (*C*), and on the *left* (*D*). Similar data were obtained in triplicate experiments. The abbreviations indicate: *Pro* (full-length), *Cl* (cleaved), and *Act* (active) caspase 3; *Tau FL*, full-length Tau; *short exp.*, short exposure; *long exp.*, long exposure. *E*, fluorescence staining with PI (*panels 1* and *2*), 6-CFDA (*panels 3* and *4*), and Hoechst (*panels 5* and *6*) of neurons treated as indicated. In *panels 5* and *6*, the nuclei of the neurons within the *white boxes* are magnified and shown on the *bottom right* of each panel. Similar results were obtained in triplicate experiments. *DIC*, differential interference contrast images.

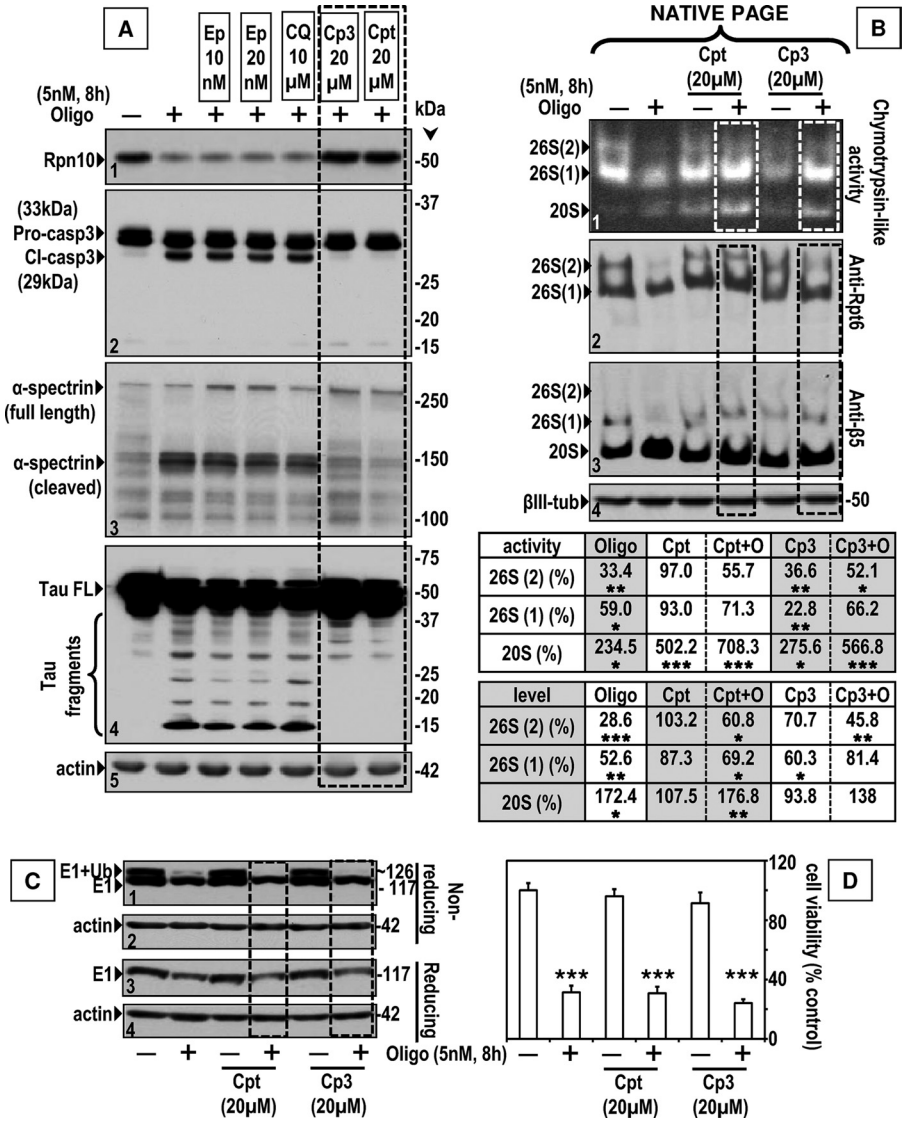

FIGURE 8. **Calpain inhibitors but not proteasome or lysosomal inhibitors prevent/diminish the effects of oligomycin on Rpn10 (*panel 1*), caspase 3 (*panel 2*), α-spectrin (*panel 3*), and Tau (*panel 4*) (*A*) and on proteasome activity (*panel 1*) and levels (*panels 2* and *3*) (*B*), but not on E1-thiol ester (*C*) and cell viability (*D*).** Rat cerebral cortical neurons were pretreated for 30 min with epoxomicin (*ep*, proteasome inhibitor), chloroquine (*CQ*, lysosomal inhibitor), Cp3 (Z-Val-Phe-CHO), and calpeptin (*Cpt*, calpain inhibitor Z-Leu-Nle-CHO) where indicated and then with oligomycin (*Oligo*). Total lysates were analyzed as follows. In *A* and *C*, by Western blotting (30 μg of protein/lane) probed with the respective antibodies using actin as loading control. In *A*, the abbreviations indicate: *panel 2*, *Pro* (full-length) and *Cl* (cleaved) caspase 3; *panel 4*, *Tau FL*, full-length Tau. In *C*, E1-ubiquitin (*E1+Ub*) thiol ester (*upper bands*) and native E1 (*lower bands*) were run under nonreducing conditions (*panels 1* and *2*) or reducing conditions with β-mercaptoethanol (*panels 3* and *4*). Molecular mass markers in kDa are shown on the *right*. Similar data were obtained in triplicate experiments. In *B*, the in-gel assay (30 μg/sample) was used to assess 26S and 20S proteasome (*indicated* on the *left* by *arrows*) chymotrypsin-like activity (*panel 1*) and levels detected by immunoblotting with anti-Rpt6 (*panel 2*) and anti-β5 antibodies (*panel 3*). *βIII-tub* indicates βIII-tubulin, used as loading control. Proteasome chymotrypsin-like activity and levels were semiquantified by densitometry (*values in tables*). The percentages represent the ratio between data for each condition and control (DMSO) considered to be 100%. Values are means from at least three experiments. *D*, cell viability was assessed with the MTT assay. The percentages represent the ratio between the data for each condition and control (100%). Values indicate means and S.E. from eight determinations per group. *Asterisks* identify values that are significantly different from control (*, $p < 0.05$; **, $p < 0.01$; ***, $p < 0.001$). *Cpt+O* and *Cp3+O*, respective calpain inhibitors plus oligomycin.

Long Term (7-Day) Incubations with Lower Doses (1 nM) of Oligomycin Mimicked the Effects of Acute (up to 16 h) Treatment with Higher (5 nM) Oligomycin Doses—In the previous experiments, we investigated the effects of short term (up to 16 h) incubations with oligomycin (5 nM). We also treated neurons with a low dose (1 nM) of oligomycin for 7 days to mimic the effect of chronic mitochondrial impairment. The same phenomena were observed upon the long 7-day treatment (Fig. 9); 26S proteasome activity (Fig. 9*A*, *panel 1*) and levels (Fig. 9*B*, *panel 1*), Ub proteins (Fig. 9*C*), and ATP (Fig. 9*D*) all declined upon oligomycin treatment. To improve detection of the 20S proteasome, 0.04% SDS was added to the activity reaction buffer at the same time as the substrate. 20S proteasome activity (Fig. 9*A*, *panel 2*) and levels (Fig. 9*B*, *panel 2*) increased concurrently with the decline in 26S proteasomes.

DISCUSSION

In this study, we characterize some of the mechanisms by which mitochondrial toxins (oligomycin, antimycin, and rotenone) affect the UPP in cortical neurons. It is clear that among the three drugs tested, rotenone caused the weakest changes on the UPP, as well as on ATP levels. In the first place, we show that

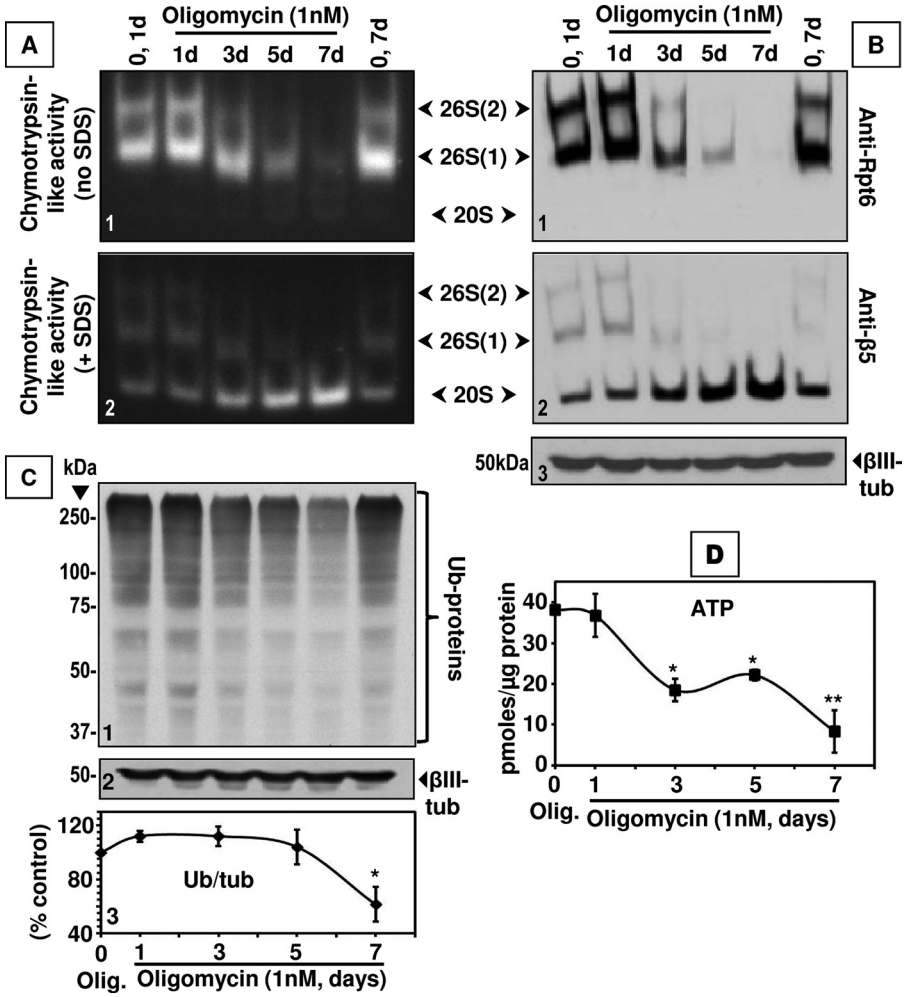

FIGURE 9. **Effects of long term incubations (up to 7 days) with oligomycin on rat cerebral cortical neurons.** Neurons were treated with oligomycin (1 nM) up to 7 days. Total lysates were analyzed by the in-gel assay (30 μg/sample) to assess 26S and 20S proteasome chymotrypsin-like activity (*panels 1* and *2*) (*A*) and levels detected by immunoblotting with anti-Rpt6 (*panel 1*), anti-β5 (*panel 2*), and anti-βIII-tubulin (β*III-tub*, loading control) antibodies (*B*). *Arrows* in the *middle* indicate assembled 26S and 20S proteasomes. *A*, *panel 2*, to improve detection of 20S proteasome activity, 0.04% SDS was added to the reaction buffer. In *C*, lysates were analyzed by Western blotting (30 μg of protein/lane) for Ub proteins. Molecular mass markers (kDa) are on the *left*. *Ub/tub*, ubiquitin/tubulin. In *D*, ATP steady state levels (pmol/μg of protein) were assessed with the luciferin/luciferase system. Controls in *C* and *D* (0, *Olig.*) represent the average between 1 and 7 days without oligomycin. Values depict the means and S.E. from at least three determinations. *Asterisks* identify values that are significantly different from control (*, $p < 0.05$; **, $p < 0.01$).

mitochondrial impairment slows down the ubiquitination cascade by blocking its first step, *i.e.* by preventing ubiquitin activation by the E1 enzyme. These results have implications for the sequence of events leading to chronic neurodegenerative diseases, such as AD, that are characterized by mitochondrial and UPP dysfunction. It is clear that these two phenomena are related in the course of AD. For therapeutic purposes, it would be important to determine which occurs upstream, UPP or mitochondrial impairment. On the one hand, our data show that treatment with the three mitochondrial inhibitors blocks the ubiquitination cascade, thus diminishing the levels of ubiquitinated proteins instead of promoting their accumulation. On the other hand, it is well established that proteasome inhibition leads to accumulation of ubiquitinated proteins and affects mitochondrial function (49, 50). Together, these data support the notion that UPP impairment may precede mitochondrial dysfunction at least in the neurodegenerative process that leads to accumulation of ubiquitinated proteins.

In the second place, we demonstrate that mitochondrial impairment provokes the demise of 26S proteasomes in neurons. 26S proteasome dysfunction is caused by its disassembly, which seems to be linked to selective processing of the Rpn10 subunit by calpain. Other proteasome subunits tested were not affected. Proteasome subunits Rpn2, Rpn10, and Rpt5 were reported to be cleaved in a caspase-mediated manner to facilitate the apoptotic program (51). Rpn10 is a subunit of the 19S regulatory particle that is a receptor for polyubiquitinated proteins (52, 53) and was recently mapped to the apex of the 26S proteasome (54). Now we show, to our knowledge for the first time, that the decline in Rpn10 upon mitochondrial deficiency is due to calpain-dependent processing as it is prevented by pretreatment with calpain inhibitors and not by proteasome or lysosomal inhibitors. Calpains do not have a strict cleavage specificity, although some preferences for particular amino acid sequences, secondary structure (disordered regions), and PEST regions were suggested (55, 56). To find a putative calpain

cleavage site on Rpn10, we used two computational programs (GPS-CCD - The Cuckoo Workgroup (57) and Calpain for Modulatory Proteolysis Database (CaMPDB) (58)). We determined that a predicted calpain cleavage site on human Rpn10 is Ala-360 (P1 position, indicated by bold and underline) within the following sequence: AIRNAMGSL**A**-SQAT.

Notably, an *rpn10* mutant that binds the proteasome but not the polyubiquitin chains rescued proteasome disassembly and loss of viability in an *rpn11-1 rpn10*Δ lethal mutant (59). Another study showed that the levels of Rpn10 are diminished in old mice, whereas those of α5 remained unchanged (60). It was postulated that the decline in Rpn10 levels could be one of the major factors responsible for decreased proteasome function occurring with aging (60). These studies further support a critical requirement for Rpn10 in proteasome assembly.

Besides Rpn10, we observed calpain-mediated cleavage of two other proteins that are relevant to AD: caspase 3 and the microtubule-associated protein Tau. Caspase 3 was cleaved to a fragment (29 kDa) that seems to be associated with caspase inactivation (55). Calpain processing of caspase 3 to an inactive form could be a measure to prevent execution of the apoptotic pathway under conditions of ATP deficit as apoptosis is an energy-dependent death pathway (61). Calpain activation is linked to ATP depletion and necrosis, a cell death pathway characterized by a bioenergetic catastrophe (61). In fact, calpain activation was shown to be induced by electron transport chain inhibitors, such as the ones used in our studies: rotenone, antimycin, and oligomycin (62).

Tau is a major component of neurofibrillary tangles in AD and other tauopathies. Tau is reported to be cleaved by caspases and/or calpain depending on the pathological condition (63). Caspase 3-induced Tau cleavage at Asp-421 has a high tendency for aggregation (45). Calpain-induced Tau fragments, including a typical 17-kDa fragment, represent a marker for enhanced calpain activity in AD (64, 65). We detected this typical 17-kDa fragment in oligomycin- and antimycin-treated neurons and observed preventive effects by calpain inhibitors. The dual vulnerability of Tau to calpain and caspases needs to be taken into consideration if preserving Tau integrity is considered as a therapeutic goal for AD and other tauopathies (63).

In the third place, we establish that mitochondrial toxins raise the activity and level of 20S proteasomes in neurons. It was proposed that 20S proteasomes in concert with immunoproteasomes degrade 70–80% of all oxidized proteins that are not aggregated (66, 67). In addition, 26S proteasomes and the ubiquitination machinery are more vulnerable to oxidative damage than 20S proteasomes (68). Because we show that mitochondrial inhibitors cause a likely decline in $\Delta\Psi_m$ and elevate ROS, it is possible that 20S proteasomes are recruited under these conditions, to promote turnover of oxidized proteins, as these proteins may not be ubiquitinated (18, 36). However, under mild conditions of oxidative stress, the UPP is up-regulated (13). Whether 26S or 20S proteasomes degrade oxidatively modified proteins remains to be confirmed.

In summary, our findings support a mechanism in neurons by which mitochondrial impairment causes a decline in the function of the ubiquitin/proteasome pathway; the steps of the ubiquitin/proteasome pathway that are energy-dependent are down-regulated, *i.e.* ubiquitin activation via E1 and 26S proteasome function. Concomitantly, 20S proteasome activity and levels are increased, possibly to promote protein degradation in a ubiquitin- and ATP-independent manner. Besides ATP depletion, calpain activation promotes the switch from 26S to 20S proteasomes as calpain processes the Rpn10 proteasome subunit. Rpn10 could act as a 26S proteasome gatekeeper to promote its disassembly when ATP is in short supply. Under low energy conditions, upgrading 20S proteasome levels and activity would ensure efficient protein degradation without energy expenditure. The reduction in ubiquitinated proteins and 26S proteasomes as well as the increase in 20S proteasomes in neurons was observed upon acute and long term mitochondrial impairment. We postulate that under acute stress conditions, unregulated protein degradation as carried out by 20S proteasomes may be sufficient to promote degradation of randomly unfolded oxidized proteins. However, regulated protein degradation by the ubiquitin/proteasome pathway is essential for long term neuronal survival.

Acknowledgments—We thank Dr. L. Binder (Northwestern University, Chicago, IL) for the Tau C5 antibody. Hunter College, City University of New York was supported by National Institutes of Health Grant G12 RR003037 (to the Gene Center at Hunter College) from the National Center for Research Resources (NCRR).

REFERENCES

1. Livnat-Levanon, N., and Glickman, M. H. (2011) Ubiquitin-proteasome system and mitochondria – reciprocity. *Biochim. Biophys. Acta* **1809,** 80–87
2. Ding, Q., Dimayuga, E., and Keller, J. N. (2006) Proteasome regulation of oxidative stress in aging and age-related diseases of the CNS. *Antioxid. Redox Signal.* **8,** 163–172
3. Stranahan, A. M., and Mattson, M. P. (2012) Recruiting adaptive cellular stress responses for successful brain ageing. *Nat. Rev. Neurosci.* **13,** 209–216
4. Reddy, P. H. (2007) Mitochondrial dysfunction in aging and Alzheimer's disease: strategies to protect neurons. *Antioxid. Redox Signal.* **9,** 1647–1658
5. Beal, M. F. (2005) Mitochondria take center stage in aging and neurodegeneration. *Ann. Neurol.* **58,** 495–505
6. Bedford, L., Paine, S., Rezvani, N., Mee, M., Lowe, J., and Mayer, R. J. (2009) The UPS and autophagy in chronic neurodegenerative disease: six of one and half a dozen of the other– or not? *Autophagy.* **5,** 224–227
7. Nicholls, D. G. (2008) Oxidative stress and energy crises in neuronal dysfunction. *Ann. N.Y. Acad. Sci.* **1147,** 53–60
8. Mosconi, L., Pupi, A., and De Leon, M. J. (2008) Brain glucose hypometabolism and oxidative stress in preclinical Alzheimer's disease. *Ann. N.Y. Acad. Sci.* **1147,** 180–195
9. Hoyer, S. (1992) Oxidative energy metabolism in Alzheimer brain. Studies in early-onset and late-onset cases. *Mol. Chem. Neuropathol.* **16,** 207–224
10. Liu, C. W., Li, X., Thompson, D., Wooding, K., Chang, T. L., Tang, Z., Yu, H., Thomas, P. J., and DeMartino, G. N. (2006) ATP binding and ATP hydrolysis play distinct roles in the function of 26S proteasome. *Mol. Cell* **24,** 39–50
11. Zhu, X., Perry, G., Smith, M. A., and Wang, X. (2013) Abnormal mitochondrial dynamics in the pathogenesis of Alzheimer's disease. *J. Alzheimers Dis.* **33,** Suppl. 1, S253–S262
12. Stadtman, E. R., and Berlett, B. S. (1998) Reactive oxygen-mediated protein oxidation in aging and disease. *Drug Metab. Rev.* **30,** 225–243
13. Shang, F., and Taylor, A. (2011) Ubiquitin-proteasome pathway and cellular responses to oxidative stress. *Free Radic. Biol. Med.* **51,** 5–16
14. Shringarpure, R., Grune, T., Mehlhase, J., and Davies, K. J. (2003) Ubiqui-

tin conjugation is not required for the degradation of oxidized proteins by proteasome. *J. Biol. Chem.* **278,** 311–318
15. Shang, F., Nowell, T. R., Jr., and Taylor, A. (2001) Removal of oxidatively damaged proteins from lens cells by the ubiquitin-proteasome pathway. *Exp. Eye Res.* **73,** 229–238
16. Lin, M. T., and Beal, M. F. (2006) Mitochondrial dysfunction and oxidative stress in neurodegenerative diseases. *Nature* **443,** 787–795
17. Dasuri, K., Ebenezer, P. J., Zhang, L., Fernandez-Kim, S. O., Uranga, R. M., Gavilán, E., Di Blasio, A., and Keller, J. N. (2010) Selective vulnerability of neurons to acute toxicity after proteasome inhibitor treatment: implications for oxidative stress and insolubility of newly synthesized proteins. *Free Radic. Biol. Med.* **49,** 1290–1297
18. Grune, T., Jung, T., Merker, K., and Davies, K. J. (2004) Decreased proteolysis caused by protein aggregates, inclusion bodies, plaques, lipofuscin, ceroid, and 'aggresomes' during oxidative stress, aging, and disease. *Int. J. Biochem. Cell Biol.* **36,** 2519–2530
19. Aiken, C. T., Kaake, R. M., Wang, X., and Huang, L. (2011) Oxidative stress-mediated regulation of proteasome complexes. *Mol. Cell. Proteomics* **10,** R110.006924
20. Grimm, S., Hoehn, A., Davies, K. J., and Grune, T. (2011) Protein oxidative modifications in the ageing brain: consequence for the onset of neurodegenerative disease. *Free Radic. Res.* **45,** 73–88
21. Brewer, G. J., Torricelli, J. R., Evege, E. K., and Price, P. J. (1993) Optimized survival of hippocampal neurons in B27-supplemented Neurobasal, a new serum-free medium combination. *J. Neurosci. Res.* **35,** 567–576
22. Nam, Y., Brewer, G. J., and Wheeler, B. C. (2007) Development of astroglial cells in patterned neuronal cultures. *J Biomater. Sci. Polym. Ed.* **18,** 1091–1100
23. Mosmann, T. (1983) Rapid colorimetric assay for cellular growth and survival: application to proliferation and cytotoxicity assays. *J. Immunol. Methods* **65,** 55–63
24. Jha, N., Kumar, M. J., Boonplueang, R., and Andersen, J. K. (2002) Glutathione decreases in dopaminergic PC12 cells interfere with the ubiquitin protein degradation pathway: relevance for Parkinson's disease? *J. Neurochem.* **80,** 555–561
25. Myeku, N., Metcalfe, M. J., Huang, Q., and Figueiredo-Pereira, M. (2011) Assessment of proteasome impairment and accumulation/aggregation of ubiquitinated proteins in neuronal cultures. *Methods Mol. Biol.* **793,** 273–296
26. Wilk, S., and Orlowski, M. (1983) Evidence that pituitary cation-sensitive neutral endopeptidase is a multicatalytic protease complex. *J. Neurochem.* **40,** 842–849
27. Degli Esposti, M. (1998) Inhibitors of NADH-ubiquinone reductase: an overview. *Biochim. Biophys. Acta* **1364,** 222–235
28. Huang, L. S., Cobessi, D., Tung, E. Y., and Berry, E. A. (2005) Binding of the respiratory chain inhibitor antimycin to the mitochondrial bc1 complex: a new crystal structure reveals an altered intramolecular hydrogen-bonding pattern. *J. Mol. Biol.* **351,** 573–597
29. Liu, Y., and Schubert, D. R. (2009) The specificity of neuroprotection by antioxidants. *J. Biomed. Sci.* **16,** 98
30. Berridge, M. V., and Tan, A. S. (1993) Characterization of the cellular reduction of 3-(4,5-dimethylthiazol-2-yl)-2,5-diphenyltetrazolium bromide (MTT): subcellular localization, substrate dependence, and involvement of mitochondrial electron transport in MTT reduction. *Arch. Biochem. Biophys.* **303,** 474–482
31. Liu, Y., Peterson, D. A., Kimura, H., and Schubert, D. (1997) Mechanism of cellular 3-(4,5-dimethylthiazol-2-yl)-2,5-diphenyltetrazolium bromide (MTT) reduction. *J. Neurochem.* **69,** 581–593
32. Rego, A. C., Vesce, S., and Nicholls, D. G. (2001) The mechanism of mitochondrial membrane potential retention following release of cytochrome *c* in apoptotic GT1–7 neural cells. *Cell Death. Differ.* **8,** 995–1003
33. Akude, E., Zherebitskaya, E., Chowdhury, S. K., Smith, D. R., Dobrowsky, R. T., and Fernyhough, P. (2011) Diminished superoxide generation is associated with respiratory chain dysfunction and changes in the mitochondrial proteome of sensory neurons from diabetic rats. *Diabetes* **60,** 288–297
34. Azzu, V., Parker, N., and Brand, M. D. (2008) High membrane potential promotes alkenal-induced mitochondrial uncoupling and influences adenine nucleotide translocase conformation. *Biochem. J.* **413,** 323–332
35. Turrens, J. F. (2003) Mitochondrial formation of reactive oxygen species. *J. Physiol.* **552,** 335–344
36. Kästle, M., and Grune, T. (2011) Proteins bearing oxidation-induced carbonyl groups are not preferentially ubiquitinated. *Biochimie* **93,** 1076–1079
37. Oddo, S. (2008) The ubiquitin-proteasome system in Alzheimer's disease. *J. Cell Mol. Med.* **12,** 363–373
38. Uchida, K., and Shibata, T. (2008) 15-Deoxy-$\Delta^{12,14}$-prostaglandin J_2: an electrophilic trigger of cellular responses. *Chem. Res. Toxicol.* **21,** 138–144
39. Shibata, T., Yamada, T., Kondo, M., Tanahashi, N., Tanaka, K., Nakamura, H., Masutani, H., Yodoi, J., and Uchida, K. (2003) An endogenous electrophile that modulates the regulatory mechanism of protein turnover: inhibitory effects of 15-deoxy-$\Delta^{12,14}$-prostaglandin J_2 on proteasome. *Biochemistry* **42,** 13960–13968
40. Jahngen-Hodge, J., Obin, M. S., Gong, X., Shang, F., Nowell, T. R., Jr., Gong, J., Abasi, H., Blumberg, J., and Taylor, A. (1997) Regulation of ubiquitin-conjugating enzymes by glutathione following oxidative stress. *J. Biol. Chem.* **272,** 28218–28226
41. Eytan, E., Ganoth, D., Armon, T., and Hershko, A. (1989) ATP-dependent incorporation of 20S protease into the 26S complex that degrades proteins conjugated to ubiquitin. *Proc. Natl. Acad. Sci. U.S.A.* **86,** 7751–7755
42. Goldberg, A. L. (2007) Functions of the proteasome: from protein degradation and immune surveillance to cancer therapy. *Biochem. Soc. Trans.* **35,** 12–17
43. Kondo, M., Shibata, T., Kumagai, T., Osawa, T., Shibata, N., Kobayashi, M., Sasaki, S., Iwata, M., Noguchi, N., and Uchida, K. (2002) 15-Deoxy-$\Delta^{12,14}$-prostaglandin J_2: the endogenous electrophile that induces neuronal apoptosis. *Proc. Natl. Acad. Sci. U.S.A.* **99,** 7367–7372
44. Wang, K. K. (2000) Calpain and caspase: can you tell the difference? *Trends Neurosci.* **23,** 20–26
45. Binder, L. I., Guillozet-Bongaarts, A. L., Garcia-Sierra, F., and Berry, R. W. (2005) Tau, tangles, and Alzheimer's disease. *Biochim. Biophys. Acta* **1739,** 216–223
46. Vitale, M., Zamai, L., Mazzotti, G., Cataldi, A., and Falcieri, E. (1993) Differential kinetics of propidium iodide uptake in apoptotic and necrotic thymocytes. *Histochemistry* **100,** 223–229
47. Breeuwer, P., Drocourt, J. L., Bunschoten, N., Zwietering, M. H., Rombouts, F. M., and Abee, T. (1995) Characterization of uptake and hydrolysis of fluorescein diacetate and carboxyfluorescein diacetate by intracellular esterases in *Saccharomyces cerevisiae*, which result in accumulation of fluorescent product. *Appl. Environ. Microbiol.* **61,** 1614–1619
48. Rinaldi, T., Ricordy, R., Bolotin-Fukuhara, M., and Frontali, L. (2002) Mitochondrial effects of the pleiotropic proteasomal mutation *mpr1*/*rpn11*: uncoupling from cell cycle defects in extragenic revertants. *Gene* **286,** 43–51
49. Sullivan, P. G., Dragicevic, N. B., Deng, J. H., Bai, Y., Dimayuga, E., Ding, Q., Chen, Q., Bruce-Keller, A. J., and Keller, J. N. (2004) Proteasome inhibition alters neural mitochondrial homeostasis and mitochondria turnover. *J. Biol. Chem.* **279,** 20699–20707
50. Papa, L., and Rockwell, P. (2008) Persistent mitochondrial dysfunction and oxidative stress hinder neuronal cell recovery from reversible proteasome inhibition. *Apoptosis* **13,** 588–599
51. Sun, X. M., Butterworth, M., MacFarlane, M., Dubiel, W., Ciechanover, A., and Cohen, G. M. (2004) Caspase activation inhibits proteasome function during apoptosis. *Mol. Cell* **14,** 81–93
52. Glickman, M. H., Rubin, D. M., Coux, O., Wefes, I., Pfeifer, G., Cjeka, Z., Baumeister, W., Fried, V. A., and Finley, D. (1998) A subcomplex of the proteasome regulatory particle required for ubiquitin-conjugate degradation and related to the COP9-signalosome and eIF3. *Cell* **94,** 615–623
53. Verma, R., Oania, R., Graumann, J., and Deshaies, R. J. (2004) Multiubiquitin chain receptors define a layer of substrate selectivity in the ubiquitin-proteasome system. *Cell* **118,** 99–110
54. Sakata, E., Bohn, S., Mihalache, O., Kiss, P., Beck, F., Nagy, I., Nickell, S., Tanaka, K., Saeki, Y., Förster, F., and Baumeister, W. (2012) Localization of the proteasomal ubiquitin receptors Rpn10 and Rpn13 by electron cryomicroscopy. *Proc. Natl. Acad. Sci. U.S.A.* **109,** 1479–1484
55. Orrenius, S., Zhivotovsky, B., and Nicotera, P. (2003) Regulation of cell

death: the calcium-apoptosis link. *Nat. Rev. Mol. Cell Biol.* **4,** 552–565
56. Sorimachi, H., and Ono, Y. (2012) Regulation and physiological roles of the calpain system in muscular disorders. *Cardiovasc. Res.* **96,** 11–22
57. Liu, Z., Cao, J., Gao, X., Ma, Q., Ren, J., and Xue, Y. (2011) GPS-CCD: a novel computational program for the prediction of calpain cleavage sites. *PLoS One* **6,** e19001
58. DuVerle, D. A., Ono, Y., Sorimachi, H., and Mamitsuka, H. (2011) Calpain cleavage prediction using multiple kernel learning. *PLoS One* **6,** e19035
59. Chandra, A., Chen, L., and Madura, K. (2010) Synthetic lethality of *rpn11–1 rpn10*Δ is linked to altered proteasome assembly and activity. *Curr. Genet.* **56,** 543–557
60. Huber, N., Sakai, N., Eismann, T., Shin, T., Kuboki, S., Blanchard, J., Schuster, R., Edwards, M. J., Wong, H. R., and Lentsch, A. B. (2009) Age-related decrease in proteasome expression contributes to defective nuclear factor-κB activation during hepatic ischemia/reperfusion. *Hepatology* **49,** 1718–1728
61. Zong, W. X., and Thompson, C. B. (2006) Necrotic death as a cell fate. *Genes Dev.* **20,** 1–15
62. Shell, J. R., and Lawrence, D. S. (2012) Proteolytic regulation of the mitochondrial cAMP-dependent protein kinase. *Biochemistry* **51,** 2258–2264
63. Liu, M. C., Kobeissy, F., Zheng, W., Zhang, Z., Hayes, R. L., and Wang, K. K. (2011) Dual vulnerability of Tau to calpains and caspase-3 proteolysis under neurotoxic and neurodegenerative conditions. *ASN. Neuro.* **3,** e00051
64. Garg, S., Timm, T., Mandelkow, E. M., Mandelkow, E., and Wang, Y. (2011) Cleavage of Tau by calpain in Alzheimer's disease: the quest for the toxic 17 kD fragment. *Neurobiol. Aging* **32,** 1–14
65. Ferreira, A., and Bigio, E. H. (2011) Calpain-mediated Tau cleavage: a mechanism leading to neurodegeneration shared by multiple tauopathies. *Mol. Med.* **17,** 676–685
66. Pacifici, R. E., Salo, D. C., and Davies, K. J. (1989) Macroxyproteinase (M.O.P.): a 670 kDa proteinase complex that degrades oxidatively denatured proteins in red blood cells. *Free Radic. Biol. Med.* **7,** 521–536
67. Pickering, A. M., Koop, A. L., Teoh, C. Y., Ermak, G., Grune, T., and Davies, K. J. (2010) The immunoproteasome, the 20S proteasome and the PA28$\alpha\beta$ proteasome regulator are oxidative-stress-adaptive proteolytic complexes. *Biochem. J.* **432,** 585–594
68. Reinheckel, T., Sitte, N., Ullrich, O., Kuckelkorn, U., Davies, K. J., and Grune, T. (1998) Comparative resistance of the 20S and 26S proteasome to oxidative stress. *Biochem. J.* **335,** 637–642